

A Targeted, Self-Delivered, and Photocontrolled Molecular Beacon for mRNA Detection in Living Cells

Liping Qiu,^{†,‡} Cuichen Wu,[‡] Mingxu You,[‡] Da Han,[‡] Tao Chen,[‡] Guizhi Zhu,^{†,‡} Jianhui Jiang,[†] Ruqin Yu,[†] and Weihong Tan^{*,†,‡}

[†]Molecular Science and Biomedicine Laboratory, State Key Laboratory of Chemo/Bio-Sensing and Chemometrics, College of Chemistry and Chemical Engineering, College of Biology, Collaborative Innovation Center for Chemistry and Molecular Medicine, Hunan University, Changsha 410082, China

[‡]Center for Research at the Bio/Nano Interface, Department of Chemistry and Department of Physiology and Functional Genomics, Shands Cancer Center, UF Genetics Institute, and McKnight Brain Institute, University of Florida, Gainesville, Florida 32611-7200, United States

S Supporting Information

ABSTRACT: The spatiotemporal dynamics of specific mRNA molecules are difficult to image and detect inside living cells, and this has been a significant challenge for the chemical and biomedical communities. To solve this problem, we have developed a targeted, self-delivered, and photocontrolled aptamer-based molecular beacon (MB) for intracellular mRNA analysis. An internalizing aptamer connected via a double-stranded DNA structure was used as a carrier probe (CP) for cell-specific delivery of the MB designed to signal target mRNA. A light activation strategy was employed by inserting two photolabile groups in the CP sequence, enabling control over the MB's intracellular function. After the probe was guided to the target cell via specific binding of aptamer AS1411 to nucleolin on the cell membrane, light illumination released the MB for mRNA monitoring. Consequently, the MB is able to perform live-cell mRNA imaging with precise spatiotemporal control, while the CP acts as both a tracer for intracellular distribution of the MB before photoinitiation and an internal reference for mRNA ratiometric detection.

The expression level and subcellular distribution of specific messenger RNA (mRNA) can be modulated by cells when responding to their internal genetic programs or external stimuli.^{1,2} Therefore, intracellular mRNA monitoring and detection can yield valuable information for biological study, medical diagnosis, adaptive therapy, and drug discovery. In this regard, live-cell imaging is a powerful approach because it promises high spatiotemporal resolution for the analysis of mRNA dynamics.^{1,3} Of the several current live-cell imaging methods for mRNA,^{3–8} molecular beacons (MBs) may be the most attractive since they are easy to make, simple to use, and not require the complicated genetic manipulations of green fluorescent protein-tagged methods.⁹ Furthermore, they have a low background without the need to wash away unbound probes as well as high multiplexing potential through labeling with different dyes. Because of their inherent signal-transduction mechanism, MBs can be used for monitoring of RNAs in real time with high sensitivity and selectivity.¹⁰ To visualize and track mRNA in specific living cells with high spatiotemporal

resolution, the probe must initially meet two important requirements: specific delivery into the target cell's cytoplasm, and good spatial and temporal resolution of the probe.

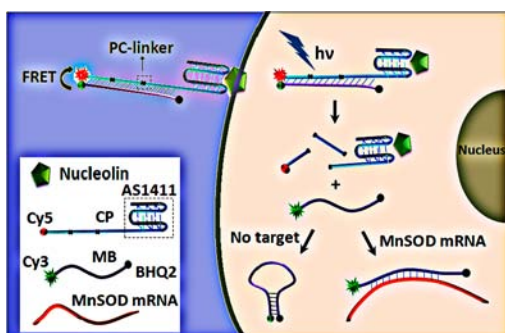
MBs are negatively charged hydrophilic macromolecules; as such, they cannot freely permeate the lipophilic cell membrane.¹¹ To solve the problem of MB delivery, several methods have been attempted, such as microinjection, transfection using liposomes and cationic polymers, and peptide-assisted delivery.¹² Despite wide investigation, all of these methods have their limitations. For example, microinjection is tedious and invasive with low throughput and fast nuclear sequester of oligonucleotides. Although peptide-assisted delivery can deliver probes efficiently, the necessary conjugation between the peptide and the DNA makes probe synthesis complicated and costly. More importantly, most of the methods reported to date show no cell specificity.

Thus, alternative delivery strategies with the advantages of high throughput, cell-type specificity, low cost, and facile preparation are being sought. Aptamers, single-stranded oligonucleotides selected through an *in vitro* method known as SELEX, have attracted much attention in biological research because of their intrinsic advantages of high affinity and selectivity, simple synthesis, and good stability.¹³ Particularly, those aptamers that can be internalized directly into cells have been widely used for targeted drug delivery.¹⁴ As nucleic acids, aptamers can easily be integrated with MBs through hybridization or one-pot synthesis in the DNA/RNA synthesizer. In addition, it has been reported that specific protein/aptamer binding can protect the DNA strand from enzymatic degradation, which would be valuable for studying living systems with DNA probes.¹⁵ Surprisingly, the incorporation of internalizing aptamers into MBs for living cell assays has not been reported to date.

Once the MB is internalized into the cytoplasm by specific aptamer binding with its target cell, it is necessary to achieve spatiotemporal control of the probe's function. The synthesis and degradation of mRNAs as well as their subcellular sorting and location are finely timed and tightly organized in living

Received: June 26, 2013

Published: August 9, 2013

Scheme 1. Schematic Illustration of the CP/MB Probe for Spatiotemporal MnSOD mRNA Detection in Living Cells^a

^aThe CP/MB probe enters the cell via specific binding of aptamer AS1411 to nucleolin on the cell membrane. Because of the more stable hybridization with the CP, the MB is inert. However, upon light illumination, the MB is released, and its ability to signal the target is restored.

cells.^{1,16} For example, the *bicoid* mRNA is concentrated at the anterior tip of oocytes within the developmental stage and early embryo until the formation of blastoderm cells.¹⁷ The expression level of manganese superoxide dismutase (MnSOD) mRNA is closely related to the malignant phenotype and tumor proliferation.¹⁸ Accordingly, methods that allow us to study specific mRNAs with high temporal and spatial resolution are expected to provide more information about the mechanisms underlying these biological events. In this regard, light irradiation is a clean form of energy with the further advantages of easy, remote, and accurate control. The photodecaging strategy is a typical example, essentially because the molecular activity is masked by a photoresponsive caging group and then recovered by specific light irradiation at a designated time and location.¹⁹ With the advantages of light stimulus and high efficiency of the photodecaging reaction, this technology allows us to determine when and where to perform the desired molecular activity in living systems.

In this work, we made use of the aforementioned three key points to design and synthesize a cell-targeted, self-delivered, photocontrolled MB for spatiotemporal mRNA monitoring in living cells, using MnSOD mRNA as the model target. To achieve this goal, we used a double-stranded DNA probe. One strand is the MB, which is designed to signal the target mRNA, while the other is the internalizing aptamer AS1411²⁰ with an extended cDNA sequence, which functions as a carrier probe (CP) for the targeted cellular delivery of the MB (Scheme 1). This aptamer is known to specifically bind to nucleolin, which is commonly overexpressed on the membranes of tumor cells.²⁰ Since nucleolin shuttles between cytoplasm and nucleus, the MB, using aptamer AS1411 as its guidance system, can be translocated across the cell membrane into the cytoplasm. In contrast to single-stranded DNAs, it has been reported that the cell-uptake efficiency of antisense DNAs can be improved through delivery as double-stranded complexes.²¹ By combining the internalizing aptamer with a duplex structure, the MB should enter the cytoplasm of specific cells efficiently. Next, to exert spatiotemporal control over the detection function of MB in living cells, two photocleavable linkers (PC-linkers), each containing an *o*-nitrobenzyl moiety, were inserted into the CP sequence [Table S1 in the Supporting Information (SI)]. In the initial stage, a stable duplex structure with a protruding aptamer is formed by hybridization between the MB and CP, causing the MB to remain

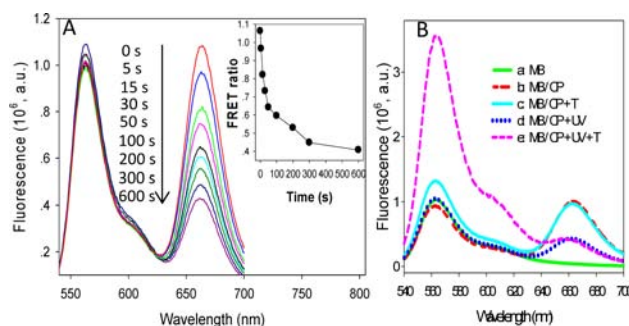


Figure 1. Photoregulation of the CP/MB probe in buffer solution. (A) Fluorescence spectra of the probe after exposure to UV light for different lengths of time. The inset shows the FRET ratio of the probe as a function of irradiation time. (B) Fluorescence spectra of the sensing system under different conditions.

in an inert state even in the presence of the target molecule (Scheme 1). However, upon irradiation with a pulse of UV light, the PC-linkers are quickly cleaved, thereby releasing the MB and activating its sensitivity to the target mRNA. In this way, the MB is guided to the target cell, enters it, and performs its detection mission at a given time and location.

Furthermore, to monitor the photocleavage process and to measure the intracellular mRNA level, the MB was modified with a Cy3 fluorophore and a BHQ2 quencher, while the CP was labeled with a Cy5 fluorophore. With this dye-labeling strategy, the photocleavage reaction could be evaluated by the change in the Förster resonance energy transfer (FRET) signal between Cy3 and Cy5. An increase in light irradiation time rapidly decreased the FRET signal of Cy5 at 663 nm, whereas the Cy3 signal at 563 nm showed little change (Figure 1A). Meanwhile, the FRET ratio, which was calculated by dividing the fluorescence intensity obtained at 663 nm by that obtained at 563 nm ($\lambda_{\text{exc}} = 525 \text{ nm}$), decreased steeply and reached a plateau after 5 min, indicating that the MB was quickly released from the CP to restore a self-quenched hairpin structure. Native polyacrylamide gel electrophoresis (PAGE) was performed to further confirm the photocleavage reaction, and it revealed cleavage of over 98% of the CPs after light irradiation for 5 min (Figure S1 in the SI). These data demonstrate that the photocleavage reaction occurs rapidly and efficiently.

To verify whether the detection of the CP/MB probe could be controlled by light, fluorescence measurements of this probe were first conducted in buffer solution (Figure 1B). Without light irradiation, only a small fluorescence enhancement of MB-Cy3 was induced by the target DNA (curve c) compared with the blank sample (curve b). Presumably, this slight increase in Cy3 signal resulted from free MBs that were not initially captured by CPs, as the FRET signal of Cy5, which represents the ratio of the CP/MB hybrids, remained unchanged. In contrast, after exposure to UV light for 10 min, the Cy3 fluorescence of the target sample increased significantly while the FRET signal of Cy5 decreased (curve e). However, under the condition of light irradiation in the absence of target, no increase in Cy3 signal was observed, and the FRET signal of Cy5 also decreased (curve d). These data prove that the inert MB can be activated to signal the presence of the target by light irradiation.

After confirming that the probe can work as expected in solution, we investigated its performance in MCF-7 cells, whose membranes overexpress nucleolin.²² First, however, several prerequisites must be satisfied before living-cell assays can be performed. Specifically, the probes should first enter the cells

efficiently and stay largely in the cytoplasm. To confirm this, CP labeled with TAMRA (CP-TMR) was used to track its intracellular location and assess its internalization ability. Confocal microscopy images showed that AS1411s were distributed throughout the cytoplasm of MCF-7 after a 2 h incubation, while the TAMRA signals from the nucleus were rather weak, as indicated in previous reports.²² The sequence- and cell type- specificity of AS1411 have been demonstrated with a control probe of random sequence (Figure S2) and a control normal bronchial epithelial cell line (HBE135, Figure S3), respectively. Meanwhile, an efficient internalization of AS1411s into MCF-7 cells was revealed by dynamic analysis (Figure S4). The cellular delivery efficiency of the double-stranded complexes (CP/unmodified MB) was higher than that of the single-stranded CP, and the exact mechanism for this is under investigation (Figure S5). Second, since unmodified oligonucleotides are usually unstable in living cells and tend to be digested by intracellular nuclease with a lifetime of ~ 30 min, it was necessary to test the stability of the probe in living cells. To accomplish this, we used a hybrid of CP-TMR with MB-Q, which had the same sequence as MB but was modified with a DABCYL quencher at its 5' end. Unexpectedly, however, after incubation for 2 h, the background signal from the cells with the CP-TMR/MB-Q probe was negligible relative to that with the CP-TMR/unmodified MB probe (Figure S6), even when the cells were kept at 37 °C with 5% CO₂ for another 4 h. This may be explained by the G-quadruplex structure of AS1411, which is able to resist enzymatic degradation,²² as well as the specific protein/ aptamer binding, which can protect the DNA sequence from exonuclease digestion.¹⁵ Finally, potential damage to the cells due to the use of UV light could be a concern. However, we found that the UV illumination conditions used in this experiment (302 nm, 1.06 W, 10 min) had no negative impact on the cells during the entire monitoring process. The cells were morphologically identical to those without UV treatment (Figure S7), and over 95% of the cells retained their viability even when irradiated for 20 min and then held at room temperature for another 2 h (Figure S8).

Having demonstrated the feasibility of using the CP/MB probe in live-cell assays, we next studied the photoactivation and mRNA detection ability of the probe in MCF-7 cells. Figure 2A presents images of cells after incubation with CP/MB probes at 37 °C for 2 h. A FRET signal of Cy5 was observed, while the Cy3 signal was negligible. After light irradiation, however, the Cy5 FRET signal disappeared and the Cy3 signal slightly increased (Figure 2B), indicating that the photodecaging reaction of the probe performed well in cells and that the basal level of endogenous MnSOD mRNA was low. As controls, cordycepin²³ and lipopolysaccharide (LPS)²⁴ were used to downregulate and upregulate the expression level of MnSOD mRNA in MCF-7 cells, respectively. Confocal fluorescence imaging was then performed (Figure 2C,D,G,H). Before light irradiation, the MBs remained in an inert state, and no detectable response signal was observed in any sample. In contrast, illumination with UV light activated the ability of the MBs to detect the target mRNA. Specifically, the sample with LPS treatment produced the highest Cy3 fluorescence signal, while the lowest Cy3 signal was observed in the sample with cordycepin treatment, compared with that treated with PBS. These results are in accord with those obtained by the traditional method (*in situ* hybridization with MBs; Figure S9), demonstrating that the expression level and distribution pattern of MnSOD mRNA in MCF-7 cells revealed by this CP/MB sensing system was not an artifact. Moreover, the fluorescence images were sharper and more vivid than those

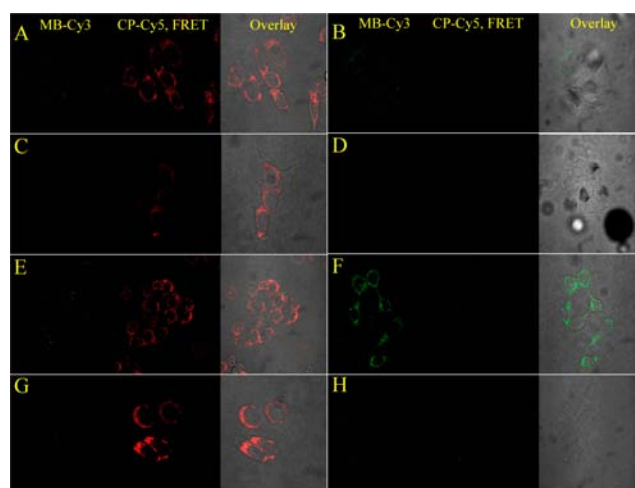


Figure 2. Confocal microscopy images of MCF-7 cells under different conditions. Cells were treated with (A, B) PBS, (C, D) 150 $\mu\text{g}/\text{mL}$ cordycepin, or (E–H) 10 $\mu\text{g}/\text{mL}$ LPS for 2 h followed by a 2 h incubation with (A–F) the CP/MB probe or (G, H) the control probe and then imaged (A, C, E, G) before and (B, D, F, H) after light irradiation. In each group, from left to right are shown the fluorescence image for Cy3, the FRET image for Cy5 under Cy3 excitation, and the overlay of the fluorescence channels and the bright-field channel.

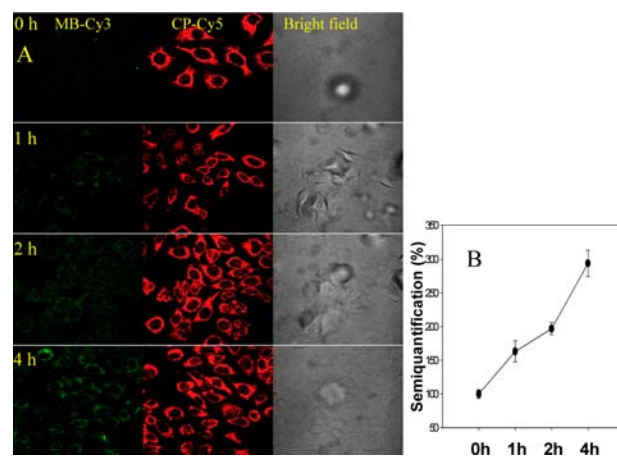


Figure 3. Ratiometric detection of MnSOD mRNA in MCF-7 cells. (A) Confocal microscopy images of MCF-7 cells with LPS stimulation for different lengths of time. From left to right are shown the MB-Cy3 and CP-Cy5 fluorescence images and the corresponding bright-field images. (B) Relative fluorescence intensities of the corresponding samples.

observed in fixed-cell assays, since a large number of the probes were constrained and opened in the nucleus during *in situ* hybridization, resulting in a high nuclear background. To demonstrate further that the signal arose solely from hybridization of the MBs with the target, a control system with the same design but having a “random” beacon with no match in the entire human genome (Table S1) was employed. No detectable Cy3 signals were observed from the LPS-stimulated samples incubated with the control probe, irrespective of light illumination (Figure 2G,H). Meanwhile, the importance of the CP for cellular delivery of the MB was confirmed by the negligible signal from the MnSOD mRNA-positive cells incubated with the MB only (Figure S10).

Since confocal microscopy can present images of only a few cells, the results of this technique will likely be skewed by the presence of experimental artifacts and cell-to-cell variation. Flow

cytometry, which is able to collect information from thousands of cells per second, was therefore used for statistical analysis of a large number of cells incubated with the target and control probes. The flow cytometry results (Figure S11) were consistent with those of confocal microscopy. Upon light irradiation, the fluorescence intensity from the sample incubated with the CP/MB probe was over 2.5 times that of the control, while each sample produced a relatively low signal without light illumination. All of these results demonstrate that the CP/MB probe is powerful for mRNA analysis in living cells.

Detection of mRNA in living cells is challenging but important for the study of cellular events. To obtain more reliable results from MBs, a strategy of ratiometric measurements is usually performed by introducing a reference probe. However, additional reference probes can increase the complexity of the sensing system. Therefore, in our scheme, the CP labeled with a Cy5 fluorophore was designed to be multifunctional. That is, the Cy5 signals not only report the amount internalized and the intracellular distribution of MBs but also serve as an internal reference for ratiometric analysis. MnSOD mRNA expression was modulated by pretreatment with LPS for different lengths of time. After removing the LPS solution, the cells were uniformly processed with the detection procedure. The Cy5 signal intensities of CP were similar with different LPS treatments (Figure 3A), indicating that this external stimulation had little impact on the internalizing ability of the probe. In contrast, the MB signal increased when LPS induction was prolonged. The imaging data were collected from these four samples and processed with NIH ImageJ software. The relative signal value was calculated by dividing F_{Cy3} by F_{Cy5} , where F_{Cy3} and F_{Cy5} represent the averaged signal intensities of Cy3 and Cy5, respectively, and the signal obtained from the sample without LPS stimulation is defined as 100%. On the basis of this CP/MB sensing system, the MnSOD mRNA expression level of MCF-7 cells treated with LPS for 1, 2, and 4 h increased to 163%, 197%, and 294%, respectively (Figure 3B), matching the results of others.²⁴ These results demonstrate that this CP/MB system is capable of detecting the target mRNA in living cells. With further photocontrollable processes and molecular engineering,^{19,20,25} one should be able to realize quantitative cellular imaging of multiple analytes in living cells.

In summary, we have developed a self-delivered MB for photoinitiated real-time imaging and detection of mRNA in living cells via direct hybridization of an extended internalizing aptamer and a molecular beacon. With this fluorescent aptamer as an internalizing carrier, the MB can be efficiently delivered into the cytoplasm of targeted cells, and its internalized amount as well as its intracellular distribution can be tracked before photoactivation. Moreover, the carrier probe can serve as an internal reference for live-cell mRNA ratiometric detection, thus eliminating the need for additional control reference probes. By means of the photocleavage reaction, this probe allows us to control the detection function of MB with high temporal resolution, while spatial resolution at the single-cell level is potentially achievable by using proper light equipment, which is valuable for studying a myriad of biological processes. Furthermore, this internalizing aptamer/detection probe system can be expanded for analysis of other biomarkers in living cells.

■ ASSOCIATED CONTENT

■ Supporting Information

Procedures and additional data. This material is available free of charge via the Internet at <http://pubs.acs.org>.

■ AUTHOR INFORMATION

Corresponding Author

tan@chem.ufl.edu

Notes

The authors declare no competing financial interest.

■ ACKNOWLEDGMENTS

L.Q. received the financial support from the China Scholarship Council. This work was supported by the National Key Scientific Program of China (2011CB911000, 2013CB933701), the Foundation for Innovative Research Groups of the NNSFC (21221003), the China National Instrumentation Program (2011YQ03012412), and NIH (GM079359, CA133086). The authors thank Dr. K. R. Williams for critical manuscript review.

■ REFERENCES

- (1) Bratu, D. P.; Cha, B.-J.; Mhlanga, M. M.; Kramer, F. R.; Tyagi, S. *Proc. Natl. Acad. Sci. U.S.A.* **2003**, *100*, 13308.
- (2) St Johnston, D. *Cell* **1995**, *81*, 161.
- (3) Tyagi, S. *Nat. Med.* **2009**, *6*, 331.
- (4) Jayagopal, A.; Halfpenny, K. C.; Perez, J. W.; Wright, D. W. *J. Am. Chem. Soc.* **2010**, *132*, 9789.
- (5) Spiller, D. G.; Wood, C. D.; Rand, D. A.; White, M. R. *Nature* **2010**, *465*, 736.
- (6) Mor, A.; Suliman, S.; Ben-Yishay, R.; Yunger, S.; Brody, Y.; Shav-Tal, Y. *Nat. Cell Biol.* **2010**, *12*, 543.
- (7) Yunger, S.; Rosenfeld, L.; Garini, Y.; Shav-Tal, Y. *Nat. Methods* **2010**, *7*, 631.
- (8) Bao, G.; Rhee, W. J.; Tsourkas, A. *Annu. Rev. Biomed. Eng.* **2009**, *11*, 25.
- (9) Wang, S.; Hazelrigg, T. *Nature* **1994**, *369*, 400.
- (10) Tyagi, S.; Kramer, F. R. *Nat. Biotechnol.* **1996**, *14*, 303.
- (11) Boussif, O.; Lezoualc'h, F.; Zanta, M. A.; Mergny, M. D.; Scherman, D.; Demeneix, B.; Behr, J.-P. *Proc. Natl. Acad. Sci. U.S.A.* **1995**, *92*, 7297.
- (12) Dokka, S.; Rojanasakul, Y. *Adv. Drug Delivery Rev.* **2000**, *44*, 35.
- (13) Shanguan, D.; Li, Y.; Tang, Z.; Cao, Z. C.; Chen, H. W.; Mallikaratchy, P.; Sefah, K.; Yang, C. J.; Tan, W. *Proc. Natl. Acad. Sci. U.S.A.* **2006**, *103*, 11838.
- (14) McNamara, J. O.; Andrechek, E. R.; Wang, Y.; Viles, K. D.; Rempel, R. E.; Gilboa, E.; Sullenger, B. A.; Giangrande, P. H. *Nat. Biotechnol.* **2006**, *24*, 1005.
- (15) Zhang, S.; Metelev, V.; Tabatadze, D.; Zamecnik, P. C.; Bogdanov, A. *Proc. Natl. Acad. Sci. U.S.A.* **2008**, *105*, 4156.
- (16) Jansen, R.-P. *Nat. Rev. Mol. Cell Biol.* **2001**, *2*, 247.
- (17) Berleth, T.; Burri, M.; Thoma, G.; Bopp, D.; Richstein, S.; Frigerio, G.; Noll, M.; Nüsslein-Volhard, C. *EMBO J.* **1988**, *7*, 1749.
- (18) Church, S. L.; Grant, J. W.; Ridnour, L. A.; Oberley, L. W.; Swanson, P. E.; Meltzer, P. S.; Trent, J. M. *Proc. Natl. Acad. Sci. U.S.A.* **1993**, *90*, 3113.
- (19) Deiters, A.; Garner, R. A.; Lusic, H.; Govan, J. M.; Dush, M.; Nascone-Yoder, N. M.; Yoder, J. A. *J. Am. Chem. Soc.* **2010**, *132*, 15644.
- (20) Cao, Z.; Tong, R.; Mishra, A.; Xu, W.; Wong, G. C.; Cheng, J.; Lu, Y. *Angew. Chem., Int. Ed.* **2009**, *48*, 6494.
- (21) Astriab-Fisher, A.; Fisher, M. H.; Juliano, R.; Herdewijn, P. *Biochem. Pharmacol.* **2004**, *68*, 403.
- (22) Soundararajan, S.; Chen, W.; Spicer, E. K.; Courtenay-Luck, N.; Fernandes, D. J. *Cancer Res.* **2008**, *68*, 2358.
- (23) Penman, S.; Rosbash, M.; Penman, M. *Proc. Natl. Acad. Sci. U.S.A.* **1970**, *67*, 1878.
- (24) Drake, T. J.; Medley, C. D.; Sen, A.; Rogers, R. J.; Tan, W. *ChemBioChem* **2005**, *6*, 2041.
- (25) Huang, F.; You, M.; Han, D.; Xiong, X.; Liang, H.; Tan, W. *J. Am. Chem. Soc.* **2013**, *135*, 7967.